that, in a 100°C mixed hydrothermal solution, the net synthesis of the amino acids constituting 1 mol of this protein releases 722 kJ. The values of ΔG_r for the net amino acid synthesis of this and eight other thermophilic proteins (Table 4) are all negative (exergonic). Combined with the conclusion that peptide bond formation is energetically favored with increasing temperature (*12*), an argument can be made that thermophilic chemoautotrophs, such as those occupying the deepest branches in the universal tree of life, expend considerably less energy for the synthesis of macromolecules, such as proteins, than do their mesophilic counterparts. Depending on the amino acid composition of the protein, the synthesis of the monomers from CO_2, H_2, and other inorganic precursors in hot, reduced aqueous solutions may provide substantial surplus energy that can be harnessed to drive intracellular synthesis of enzymes and other polymers.

Our results might start to explain the phenomenal rates of biomass production around hydrothermal vents (*21*) and also how hyperthermophilic Archaea in natural or laboratory high-temperature systems are able to synthesize all required intracellular biomolecules in time periods ranging from minutes to hours as their population doubles. Our calculations can be used as a template in concert with constraints on the flow of energy through early hydrothermal systems to determine the potential of such systems as environments where amino acid and protein synthesis, primitive metabolisms, and even the universal ancestor of all extant life emerged. Calculations representing early Earth hydrothermal systems must reflect the differences in geochemistry and geophysics from active analogs. For example, sensitivity tests show that lower O_2 concentrations in seawater and ultramafic host rocks enhance the potential for hydrothermal organic synthesis (*13*), and the same should be expected for amino acid and protein synthesis.

References and Notes

1. C. Woese, *Proc. Natl. Acad. Sci. U.S.A.* **95**, 6854 (1998).
2. E. Pennisi, *Science* **280**, 672 (1998).
3. N. R. Pace, *ibid.* **276**, 734 (1997).
4. E. L. Shock, in *Evolution of Hydrothermal Ecosystems on Earth (and Mars?)*, G. R. Bock and J. A. Goode, Eds. (Wiley, Chichester, UK, 1996), pp. 40–60.
5. M. J. Russell and A. J. Hall, *J. Geol. Soc. London* **154**, 337 (1997).
6. B. M. Jakosky and E. L. Shock, *J. Geophys. Res.*, in press.
7. C. Huber and G. Wächtershäuser, *Science* **276**, 245 (1997); *ibid.* **281**, 670 (1998).
8. E. L. Shock, T. M. McCollom, M. D. Schulte, in *Thermophiles: The Keys to Molecular Evolution and the Origin of Life?*, J. Wiegel and M. W. W. Adams, Eds. (Taylor and Francis, London, in press).
9. ———, *Origins Life Evol. Biosphere* **25**, 141 (1995).
10. T. M. McCollom and E. L. Shock, *Geochim. Cosmochim. Acta* **61**, 4375 (1997).
11. E. L. Shock, *Origins Life Evol. Biosphere* **20**, 331 (1990).
12. ———, *Geochim. Cosmochim. Acta* **56**, 3481 (1992).
13. ——— and M. D. Schulte, *J. Geophys. Res.*, in press.
14. The standard-state convention for aqueous species is unit activity in a hypothetical 1 *m* solution referenced to infinite dilution at any temperature and pressure, and the standard-state convention for H_2O is unit activity of the pure component at any temperature and pressure.
15. The convention for ΔG_f° is to use the standard Gibbs free energy of formation from the elements at 25°C and 1 bar (ΔG_f°) and to integrate from there in temperature and pressure. Because the properties of the elements will cancel in any reaction, using values of ΔG_f° at high temperatures and pressures eliminates the need to calculate the high-temperature and high-pressure values of the standard Gibbs free energies of the elements.
16. H. C. Helgeson, D. H. Kirkham, G. C. Flowers, *Am. J. Sci.* **281**, 1249 (1981); E. L. Shock and H. C. Helgeson, *Geochim. Cosmochim. Acta* **52**, 2009 (1988); ———, D. A. Sverjensky, *ibid.* **53**, 2157 (1989); E. L. Shock, E. H. Oelkers, J. W. Johnson, D. A. Sverjensky, H. C. Helgeson, *J. Chem. Soc. Faraday Trans.* **88**, 803 (1992); J. P. Amend and H. C. Helgeson, *Geochim. Cosmochim. Acta* **61**, 11 (1997); *J. Chem. Soc. Faraday Trans.* **93**, 1927 (1997); E. L. Shock, D. C. Sassani, M. Willis, D. A. Sverjensky, *Geochim. Cosmochim. Acta* **61**, 907 (1997).
17. J. W. Johnson, E. H. Oelkers, H. C. Helgeson, *Comput. Geosci.* **18**, 899 (1992).
18. Because the activities of amino acids in vent fluids are not currently known, we set the activity values to zero. This assumption will introduce only minimal error in mixed hydrothermal solutions unless the concentrations of free amino acids in 350°C vent fluids are substantially higher than the concentrations in seawater.
19. D. E. Ingmanson and M. J. Dowler, *Origins Life Evol. Biosphere* **8**, 221 (1977); J. A. Baross and S. E. Hoffman, *ibid.* **15**, 327 (1985); G. Wächtershäuser, *Syst. Appl. Microbiol.* **10**, 207 (1988).
20. To determine Z_C (*22*) in an amino acid, the sum of the nominal oxidation states for each carbon atom is divided by the total number of carbon atoms in the compound. A carbon atom is assigned a nominal charge of −1 for each bond to a hydrogen atom; 0 for each bond to another carbon atom; and +1 for each bond to an oxygen, nitrogen, or sulfur atom.
21. R. A. Lutz *et al.*, *Nature* **371**, 663 (1994).
22. H. C. Helgeson, *Can. Mineral.* **29**, 707 (1991).
23. At the temperatures and pHs of the two environments considered here, 16 of the 20 amino acids have a net charge of 0, 2 are present as anions (aspartate$^-$ and glutamate$^-$), and 2 are cations (arginine$^+$ and lysine$^+$).
24. K. L. Von Damm, *Annu. Rev. Earth Planet. Sci.* **18**, 173 (1990).
25. M. Lilley, personal communication.
26. T. Takahashi, W. S. Broecker, A. E. Bainbridge, R. F. Weiss, *Tech. Rep. CU-1-80* (Lamont-Doherty Geological Observatory, Palisades, NY, 1980).
27. Although likely to be lower, the activities of amino acids in deep seawater are conservatively estimated to be equal to the activities of amino acids in surface seawater.
28. R. G. Keil, in preparation.
29. P. R. Blake *et al.*, *Biochemistry* **30**, 10885 (1991).
30. S. C. Busse *et al.*, *ibid.* **31**, 11952 (1992).
31. V. Schultes, R. Deutzmann, R. Jaenicke, *Eur. J. Biochem.* **192**, 25 (1990).
32. A. M. Engel, Z. Cejka, A. Lupas, F. Lottspeich, W. Baumeister, *EMBO J.* **11**, 4369 (1992).
33. M. Bachleitner, W. Ludwig, K. O. Stetter, K. H. Schleifer, *FEMS Microbiol. Lett.* **57**, 115 (1989).
34. A. M. Sanangelantoni, G. Forlani, F. Ambroselli, P. Cammarano, O. Tiboni, *J. Gen. Microbiol.* **138**, 383 (1992).

35. We thank two anonymous reviewers for their insightful critique of an earlier version of this manuscript and H. Helgeson, G. Olsen, R. Keil, M. Lilley, T. McCollom, M. Schulte, J. Deming, J. Baross, M. Summit, A. Playsunov, M. Zolotov, P. Prapaipong, and G. Chan for many helpful discussions. Financial support was provided by NSF grant OCE-9714288 and by NASA grant NAG5-4002. This is GEOPIG contribution 162.

22 May 1998; accepted 3 August 1998

Crystal Structure of the Catalytic Domain of Human Plasmin Complexed with Streptokinase

Xiaoqiang Wang, Xinli Lin, Jeffrey A. Loy, Jordan Tang, Xuejun C. Zhang*

Streptokinase is a plasminogen activator widely used in treating blood-clotting disorders. Complexes of streptokinase with human plasminogen can hydrolytically activate other plasminogen molecules to plasmin, which then dissolves blood clots. A similar binding activation mechanism also occurs in some key steps of blood coagulation. The crystal structure of streptokinase complexed with the catalytic unit of human plasmin was solved at 2.9 angstroms. The amino-terminal domain of streptokinase in the complex is hypothesized to enhance the substrate recognition. The carboxyl-terminal domain of streptokinase, which binds near the activation loop of plasminogen, is likely responsible for the contact activation of plasminogen in the complex.

The activation of human plasminogen (Plg) to plasmin (Pm) in blood plasma is the central event that results in the dissolution of the fibrin clot by proteolysis. Human Plg, a single-chain protein of 791 residues, contains five kringle domains and a serine protease domain (*1*). Plg activation by physiological activators, for example, tissue-type plasminogen activator (TPA), is accomplished by the hydrolysis of the Arg^{561}-Val^{562} bond in Plg (*2*). Plg activators, TPA and streptokinase (SK), are widely used as thrombolytic agents

for treatments of blood-clotting disorders, such as acute myocardial infarction. SK is a 414-residue protein secreted by hemolytic strains of Streptococci (*3*). Unlike TPA, SK is not a protease. It forms a stoichiometric complex with either Plg or Pm. The complexes can hydrolytically activate other Plg molecules, a property endowed to neither Plg nor Pm alone (*4*). This mechanism of zymogen activation by tight protein-protein binding is shared with staphylokinase (SAK), a staphylococcal Plg activator (*5*), and several key proteins in blood coagulation (*6*). However, only limited structural information is available on such systems. Both Plg and SK are made up of multiple domains (*7*), which account for the difficulty in crystallizing them for structural studies. The catalytic domains of Plg (that is, the region of residues 542 to 791) and Pm are commonly called microplasminogen (μPlg) and microplasmin (μPm), respectively. Because μPlg can bind and be activated by SK (*8*), it should contain the essential structural information for understanding SK activation. The strategy we devised for recombinant production of the proteins and successful crystallization (*9*) of μPlg complexed to SK included (i) the replacement of the active-site residue Ser^{741} with Ala to reduce the autolysis of the complex and (ii) the formation of the complex by refolding of recombinant μPlg and SK concomitantly. During the crystallization process, some low-level proteolytic activity cleaved SK and also converted μPlg to μPm (*10*). The x-ray diffraction data of the crystal were collected up to 2.9 Å. The structural solution was obtained mainly with the multiple isomorphous replacement (MIR) method (*11*). (Table).

The catalytic domain of Pm has dimensions of about 40 Å × 45 Å × 50 Å. Its overall structure is similar to that of other trypsin-family enzymes. For example, the coordinate root-mean-square deviation (rmsd) between μPm and the two-chain TPA (*12*) is 0.74 Å for 177 C_α atoms (with a 1.5 Å cutoff). μPm consists of two six-stranded β barrels and a COOH-terminal α helix (Fig. 1). The electron density of the active-site residues confirmed the Ser^{741} to Ala substitution. Four Pm-specific NH_2-terminal residues, Val-Val-Gly-Gly (residues 562 to 565), are accommodated in the activation pocket and are stabilized by a solvent-inaccessible salt bridge between the amino group of the NH_2-terminus and the carboxylate group of Asp^{740}. It is well known that the conformational change induced by this salt bridge is responsible for the formation of catalytic elements including the oxyanion hole and the S_1 specificity pocket (*13*). Among the six disulfide bonds in the μPm structure, the Cys^{558}-Cys^{566} pair is unique to Plg and Pm. This disulfide bond knots the seven-residue activation loop in Plg and possibly constrains the loop conformation for activation specificity. A genetic clotting disorder is linked to a mutation of Ala^{601}, whose side chain tightly packs against the imidazole ring of active-site His^{603}. The larger mutant Thr^{601} side chain (*14*) would seriously disrupt the essential hydrogen bond between His^{603} and Asp^{646}, thus impairing the catalytic mechanism.

SK appears in the complex as three domains (beginning at the NH_2-terminus, the α, β, and γ domains) of similar folding, separated by two coiled coils (Fig. 1). Domains α and β each contain a major β sheet of five mixed β strands and an α helix, a typical structure of the β grasp folding class (*15*). The coordinate rmsd between these two domains is 1.7 Å for 81 residues (with a 4.0 Å cutoff). The γ domain has only four β strands and contains a long coiled coil segment instead of an α helix. The functionally dispensable terminal regions, that is, the NH_2-terminal 15 and the COOH-terminal 32 residues (*16*), are among the several disordered regions. Others include residues 46 to 70 in the α domain and two short stretches in the β domain.

The extent of interactions of the SK domains with μPm in the complex is in the

Table 1. Summary of data collection, data statistics, and MIR phasing.

Data set	Resolution (Å)	Complete (%)	No. of reflections	R_{sym}*	R_{iso}†	⟨PP⟩‡ acen/cen	Major sites
Native§	2.9	91	33,424	0.05	–	–	–
K_2PtCl_4	3.6	94	18,287	0.08	0.21	1.22/0.76	6
$K_2Pt(NO_2)_4$	3.0	91	30,246	0.09	0.24	1.31/0.86	9
$C_7H_5HgO_3$·Na‖	3.6	93	18,221	0.12	0.18	0.92/0.75	3
Pt&Hg¶	3.2	82	22,873	0.09	0.26	1.14/0.73	8
$K_2Pt(CNS)_6$	3.4	95	21,955	0.10	0.24	1.07/0.67	8
K_2PtCl_6	3.0	92	31,176	0.08	0.27	1.80/0.93	9
K_3IrCl_6	3.4	91	20,869	0.08	0.19	0.54/0.45	2
FOM# (3.4 Å)		0.60					

*$R_{sym} = \Sigma_{hkl}|I - \langle I\rangle|/\Sigma I$, where I is the observed intensity and $\langle I\rangle$ is the average intensity from observations of symmetry-related reflections. †$R_{iso} = \Sigma_{hkl}||F_{PH}| - |F_P||/\Sigma(|F_{PH}| + |F_P|)$, where F_P and F_{PH} are the structure factor amplitudes from the protein and the heavy atom derivative, respectively. ‡⟨PP⟩ acen/cen: the phasing power for both acentric and centric reflections. §All heavy-atom soaking experiments were performed in the standard mother liquor of 1.2 M sodium citrate, 0.2 M Hepes (pH 8.0), and 1% glycerol (v/v). ‖*p*-Hydroxy-mercury-benzoate. ¶Soaked in 1.4 mM K_2PtCl_4 for 1 day followed by soaking in saturated *p*-hydroxy-mercury-benzoate for 4 days. #FOM: figure of merit.

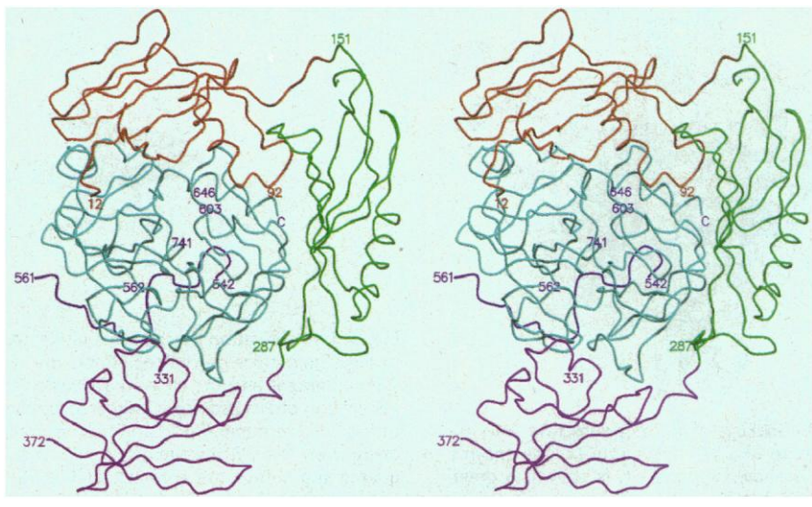

Fig. 1. Stereoview of the crystal structure of human μPm-SK complex in C_α traces. The μPm molecule is shown in blue with the NH_2-terminal short peptide in dark blue. The α, β, and γ domains of SK are shown in yellow, green, and purple, respectively. The chymotrypsin equivalences of the labeled μPm residues are 15 (561 in Pm), 16 (562), 57 (603), 102 (646), and 195 (741).

X. Wang and X. C. Zhang, Crystallography Program, Oklahoma Medical Research Foundation, 825 N.E. 13th Street, Oklahoma City, OK 73104, USA. X. Lin, Protein Studies Program, Oklahoma Medical Research Foundation, 825 N.E. 13th Street, Oklahoma City, OK 73104, USA. J. A. Loy and J. Tang, Protein Studies Program, Oklahoma Medical Research Foundation, 825 N.E. 13th Street, Oklahoma City, OK 73104, USA, and Department of Biochemistry and Molecular Biology, University of Oklahoma Health Sciences Center, 940 Stanton L. Young Street, Oklahoma City, OK 73104–5042, USA.

*To whom correspondence should be addressed. E-mail: zhangc@omrf.ouhsc.edu

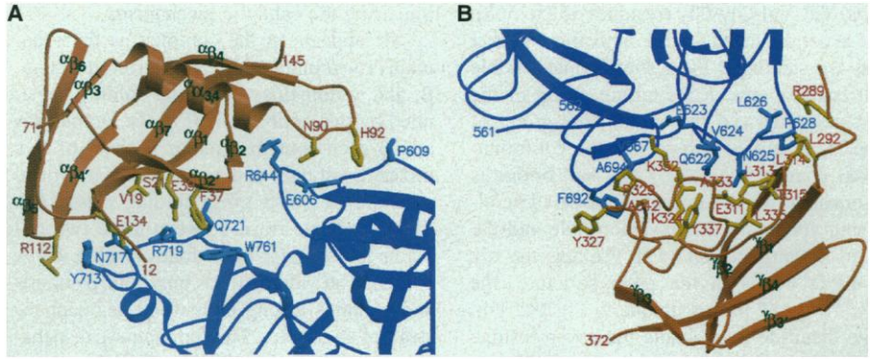

Fig. 2. Interactions between human μPm and the (**A**) α and (**B**) γ domains of SK. μPm is shown in blue and SK in orange. The side chains involved in the interactions are also shown as stick models and labeled. Also labeled are the secondary structures in the SK α and γ domains. Abbreviations for the amino acid residues are as follows: A, Ala; D, Asp; E, Glu; F, Phe; H, His; K, Lys; L, Leu; N, Asn; P, Pro; Q, Gln; R, Arg; S, Ser; T, Thr; V, Val; W, Trp; and Y, Tyr.

descending order α, γ, and β, with 1650, 1500, and 950 Å^2, respectively, of buried interfaces between each domain and μPm. The SK α domain binds to μPm mainly through interactions between the $^{\alpha}\beta_1$ and $^{\alpha}\beta_2$ strands of SK and a loop region (residues 713 to 721) of μPm (Fig. 2A), in which μPm Arg^{719} (*17*) forms salt bridges to SK Glu^{39} and Glu^{134} and has a van der Waals contact to SK Val^{19} (*18*). The SK α domain also interacts with Plg near the catalytic triad residues His^{603} and Asp^{646}. The mode of interaction between SK α domain and μPm differs from those involving the other β grasp folding proteins, which is primarily β sheet formation (*19*).

The SK γ domain binds to μPm near the activation cleavage site of Plg (Fig. 2B). Extensive charged and hydrophobic interactions are seen. Taking part on the μPm side are the "calcium-binding loop" (residues 622 to 628) and the "autolysis loop" (residues 692 to 695) and on the SK side are the major coiled coil region and the strands $^{\gamma}\beta_1$ and $^{\gamma}\beta_2$. The participation of the calcium-binding loop in this interaction suggests that the substantial sequence difference observed in this region between human and bovine Plg may contribute to the inability of SK to activate the latter. There is no direct interaction of SK with the μPm "activation loop" (residues 558 to 566). The closest interaction involves μPlg Val^{567} and SK Ala^{342}.

The interaction of the SK β domain with μPm in this structure is relatively meager. However, the current model does not exclude the possibility that the β domain may directly interact with the kringles of Plg in the activator complex and with the substrate Plg. The average crystallographic thermal factor is 80 Å^2 for the SK β domain, compared with 29, 48, and 43 Å^2 for μPm, the SK α domain, and the SK γ domain, respectively. This mobility is apparently due to the absence of crystal contact between the SK β domain and symmetry-related protein molecules.

The structure of the SK-μPm complex provides insight into how the binding of SK extends the activity of Pm from fibrin hydrolysis to Plg activation. A view into the active site of the complex reveals the concave surface of a "three-sided crater," with the active site of μPm on the crater floor and SK forming the crater rim. Docking of a model of the μPlg substrate, with its activation bond Arg^{561}-Val^{562} positioned in the catalytic site of the μPm-SK complex, results in extensive contacts between the μPlg substrate and the three domains of SK on the rim (Fig. 3). The substrate μPlg interacts most extensively with the enzyme μPm and the SK α domain and least with the SK γ domain. Not only is the size of the SK rim nearly a perfect fit for the substrate, but also regional interactions are rational. These regional interactions include several potential salt bridges, hydrogen bonds between the $^{\beta}\beta_2$ strand of SK and residues 625 to 629 of the substrate Plg, and a projected interaction between the mobile region of residues 45 to 50 in SK (*20*) and kringle 5 of the substrate Plg. Kinetic data are

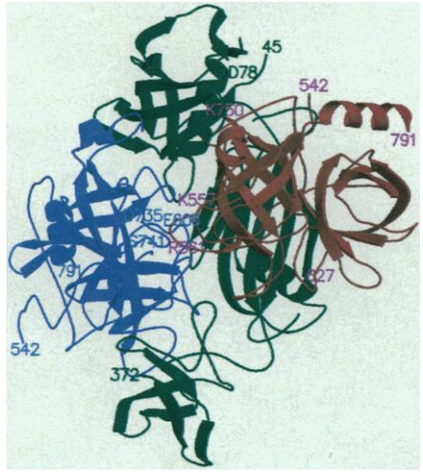

Fig. 3. Docking of a μPlg substrate into the active site of a SK-μPm complex. The enzyme, μPm, is shown in blue, SK is shown in green, and the substrate, μPlg, is shown in red. Selected residues, including the active-site residue, Ser^{741}, from the enzyme and the activation bond P_1 residue, Arg^{561}, from the substrate, are labeled.

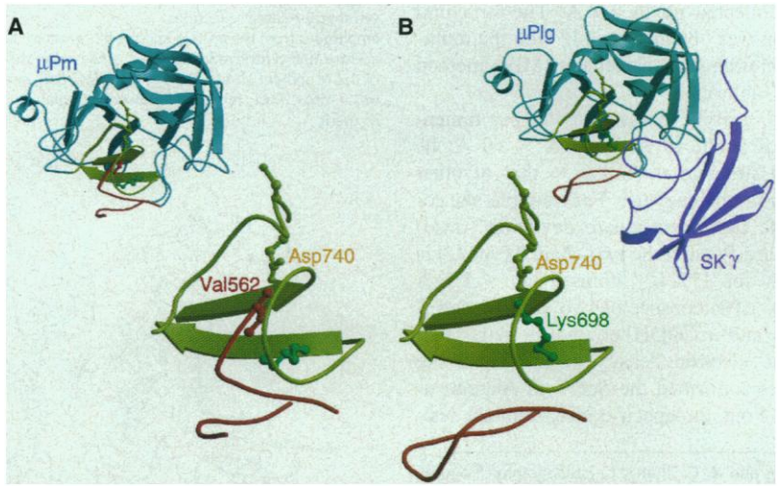

Fig. 4. Two activation mechanisms of Plg. (**A**) Structural basis of activation by proteolytic cleavage of Plg. The picture on the top shows the structure of μPm (blue) in which the activation pocket (yellow-green) and the cleaved activation loop (red) are enlarged below. In this mechanism, the generation of Pm activity is triggered by the formation of a salt bridge between the amino group of the NH_2-terminal Val^{562} and the carboxyl group of Asp^{740}. The Lys^{698} side chain (green) points away from the salt linkage. (**B**) A hypothetical model for binding activation of μPlg. The picture on the top shows the complex of the SK γ domain (magenta) with μPlg (blue) in which the important region is enlarged below. In this activation mechanism, the activation loop (red) is uncleaved. The binding of the SK γ domain in the vicinity of the activation loop is hypothesized to change the side chain position of residue Lys^{698} (green), which forms a salt linkage to Asp^{740} and triggers the activation of catalysis. Note the structural similarity of the salt linkages in (A) and (B).

consistent with the idea that Plg activation by the Pm-SK complex is assisted by additional interactions provided by SK. Although the Michaelis constant (K_m) values for the small substrate D-Val-Leu-Lys-*p*-nitroanilide are 1.3 mM for Pm and 0.5 mM for the SK-Pm complex, the K_m value of Plg activation by the SK-Pm complex is 0.15 μM (*21*). This strong interaction is supported by a very stable activation complex of Plg and SK, which has a dissociation constant near 1 nM (*22*). Furthermore, synthetic internally disulfide-linked cyclic peptides, containing the activation loop sequence of Plg, are not cleaved by TPA (*23*). The implication is that, in a Plg substrate, the conformation of this loop is strained so that a strong interaction of Plg substrate with either SK-Plg or TPA may be required to make it susceptible to hydrolysis.

How does SK activate Plg by binding to it? The most plausible hypothesis resulting from the SK-μPm structure is that binding of the SK γ domain induces a conformational change in the activation pocket of Plg. The equivalent region in a typical trypsinogen-like zymogen is known to undergo a conformational change upon the activation cleavage (*13*). Among the trypsin-like serine protease family, a few zymogens, for example, TPA (*24*) and vampire-bat Plg activator (*25*), are intrinsically active. In the crystal structure of TPA, an essential Lys^{156} residue (*26*) forms a salt linkage in the activation pocket at a position equivalent to that occupied by the NH_2-termini of activated serine proteases. In the SK-μPm complex, the activation pocket contains the NH_2-terminal Val^{562}, which forms the critical salt linkage to Asp^{740}. However, a lysine residue at position 698 is located in the activation pocket in such a way that it can replace Val^{562} to form the salt linkage in the absence of the latter (Fig. 4). The model of such a replacement produces a structure virtually identical to the same region of TPA. These comparisons suggest that, in a Pm or a free Plg molecule, the side chain of Lys^{698} stays away from Asp^{740} (Fig. 4A). The binding of the SK γ domain to the autolysis loop region of Plg may cause a conformational change of Lys^{698}, resulting in the formation of the critical salt linkage (Fig. 4B) and thereby the activation of Plg catalytic apparatus.

The contact activation system most similar to SK-mediated Plg activation is Plg activation by SAK, which is only one-third the size of SK. There is no detectable sequence homology between them. The crystal structure of SAK (*27*), however, is similar to that of the SK α domain but less so to that of the SK γ domain. The coordinate rmsd between the α domain and SAK is 1.8 Å for 91 C_α atoms (with a 4.0 Å cutoff). The structural similarity of SAK and the SK α domain suggests that they may bind to the same site on Plg or Pm. Assuming a function analogous to that of the SK α domain, the SAK moiety in a SAK-Pm complex should provide substrate recognition and thus be able to activate the Plg substrate. An extension of this line of reasoning would also predict that the SAK-Plg complex cannot activate Plg substrate because of the lack of the γ domain to activate Plg moiety in the complex. This hypothesis is supported by the following observations: (i) the activation of Plg by SAK requires the preexisting Pm (*28*), (ii) SAK and the SK α domain share the same target region on the Plg surface (*17*, *29*), and (iii) some structurally equivalent residues in SAK and SK are functionally similar (*18*, *30*).

References and Notes

1. L. Sottrup-Jensen, H. Claeys, M. Zajdel, T. E. Petersen, S. Magnusson, *Program Chem. Fibrinolysis Thrombolysis* **3**, 191 (1978); T. E. Petersen, M. R. Martzen, A. Ichinose, E. W. Davie, *J. Biol. Chem.* **265**, 6104 (1990).
2. F. Bachmann, in *Hemostasis and Thrombosis: Basic Principles and Clinical Practice*, R. W. Coleman, J. Hirsh, V. J. Marder, E. W. Salzman, Eds. (Lippincott, Philadelphia, PA, 1994), pp. 1592–1622.
3. K. W. Jackson and J. Tang, *Biochemistry* **21**, 6620 (1982); H. Malke, B. Roe, J. J. Ferretti, *Gene* **34**, 357 (1985).
4. F. J. Castellino, *Trends Biochem. Sci.* **4**, 1 (1979).
5. D. K. McClintock and P. H. Bell, *Biochem. Biophys. Res. Commun.* **43**, 694 (1971); T. Trieu, D. Behnke, D. Gerlach, J. Tang, *Methods Enzymol.* **223**, 156 (1993).
6. R. A. DeLa Cadena, Y. Wachtfogel, R. W. Colman, in *Hemostasis and Thrombosis: Basic Principles and Clinical Practice*, R. W. Coleman, J. Hirsh, V. J. Marder, E. W. Salzman, Eds. (Lippincott, Philadelphia, PA, 1994), pp. 219–240; C. L. Villiers, G. J. Arlaud, M. G. Colomb, *Proc. Natl. Acad. Sci. U.S.A.* **82**, 4477 (1985).
7. F. Conejero-Lara *et al.*, *Protein Sci.* **5**, 2583 (1996); L. V. Medved, D. A. Solovjov, K. C. Ingham, *Eur. J. Biochem.* **239**, 333 (1996); P. Rodriguez *et al.*, *ibid.* **229**, 83 (1995); K.-C. Young *et al.*, *J. Biol. Chem.* **273**, 3110 (1998).
8. G. Y. Shi, B. I. Chang, D. H. We, Y. M. Ha, H. L. Wu, *Thromb. Res.* **58**, 317 (1990).
9. Recombinant SK and μPlg were expressed from pET11 vector (Novagen, Madison, WI) with *Escherichia coli* strain BL21 (DE3) as host. The recovery, washing, and solubilization of inclusion bodies of SK and μPlg were similar to previously described procedures [X. L. Lin, Y. Z. Lin, J. Tang, *Methods Enzymol.* **241**, 195 (1994)]. The mixed solution of the two proteins, in 8 M urea, 0.1 M tris (pH 8.5), 1 mM glycine, 1 mM EDTA, and 0.1 M β-mercaptoethanol, was refolded with the rapid dilution method, followed by chromatography purification with a Sephacryl S-300 column. Crystals were grown at 20°C from sitting drops of protein solution (40 mg/ml) mixed 1:1 with the reservoir solution in vapor diffusion plates, where the reservoir solution was 1.0 M sodium citrate, 0.2 M Hepes (pH 8.0), and 1 mM magnesium chloride. The crystals had a typical size of 0.1 mm × 0.1 mm × 0.5 mm. The space group is $P2_1$, with cell parameters of $a = 80.0$ Å, $b = 125.1$ Å, $c = 86.8$ Å, and $\beta = 105.4°$. One crystallographic asymmetric unit contains two essentially identical SK-μPm complexes.
10. The protein content of the crystals was analyzed by SDS–polyacrylamide gel electrophoresis and NH_2-terminal sequence determination. Four SK-related bands appeared as the result of a complete cleavage between Lys^{59} and Ser^{60} and a partial cleavage between Lys^{258} and Ser^{259}. Two μPlg bands were the result of a cleavage between Arg^{561} and Val^{562}. The correct activation cleavage specificity in μPlg suggests that a low level of proteolytic activity had been restored from the low incidence of ribosome translation error [P. Schimmel, *Acc. Chem. Res.* **22**, 232 (1989); X. L. Lin, M. Fusek, J. Tang, *Adv. Exp.. Med. Biol.* **306**, 255 (1991)].
11. Diffraction data were collected on a Siemens area detector at room temperature. Molecular replacement with chymotrypsin [M. Harel, C. T. Su, F. Frolow, I. Silman, J. L. Sussman, *Biochemistry* **30**, 5217 (1991)] as a search model established a local twofold symmetry. The MIR phases were solved with the programs SOLVE [T. C. Terwilliger and J. Berendzen, *Acta Crystallogr. D* **52**, 749 (1996)] and MLPHARE [Z. Otwinowsky, in *Isomorphous Replacement and Anomalous Scattering, Proceedings of the CCP4 Study Weekend*, W. Wolf, P. R. Evans, A. G. W. Leslie, Eds. (SERC Daresbury Laboratory, Warrington, UK, 1991), pp. 80–86] (see Table 1). The initial MIR phases were improved by electron density averaging over the twofold noncrystallographic symmetry and solvent flattening with the program DM [K. D. Cowtan and P. Main, *Acta Crystallogr. D* **52**, 43 (1996)]. Model building from the electron density map was done with the program O [T. A. Jones, J. Y. Zou, S. W. Cowan, M. Kjelgaard, *Acta Crystallogr. A* **47**, 110 (1991)]. The program SigmaA [R. J. Read, *ibid.* **42**, 140 (1986)] was used to combine phase information at initial stages of model building. Refinement was carried out with the program X-PLOR version 3.8 [A. T. Brünger, J. Kuriyan, M. Karplus, *Science* **235**, 458 (1987)]. Non–crystallographic-symmetry constraints were used throughout the refinement. At late stages of the refinement, both grouped temperature factor refinement and a bulk solvent correction were applied. The final R factor is 21.5% over the 20.0 to 2.9 Å resolution shell (29,980 reflections), and the free R [A. T. Brünger, *Nature* **355**, 472 (1992)] is 29.2% (3330 reflections). Bond and angle deviations are 0.009 Å and 1.57°, respectively. Structural superposition and solvent-accessible surface calculation were carried out with the program EDPDB [X. Zhang and B. W. Matthews, *J. Appl. Crystallogr.* **28**, 624 (1995)]. Figures in this manuscript were created with MOLSCRIPT and RASTER3D [P. J. Kraulis, *J. Appl. Crystallogr.* **24**, 946 (1991); E. A. Merritt and M. E. P. Murphy, *Acta Crystallogr. D* **50**, 869 (1994)]. The coordinates of the complex have been deposited in the Brookhaven Protein Databank (1BML).
12. D. Lamba *et al.*, *J. Mol. Biol.* **258**, 117 (1996).
13. S. T. Freer, J. Kraut, J. D. Robertus, H. T. Wright, N. H. Xuong, *Biochemistry* **9**, 1997 (1970).
14. A. Ichinose *et al.*, *Proc. Natl. Acad. Sci. U.S.A.* **88**, 115 (1991).
15. A. G. Murzin *et al.*, *J. Mol. Biol.* **247**, 536 (1995).
16. K. W. Jackson, H. Malke, D. Gerlach, J. J. Ferretti, J. Tang, *Biochemistry* **25**, 108 (1986); K.-C. Young *et al.*, *J. Biol. Chem.* **270**, 29601 (1995).
17. K. M. Dawson *et al.*, *Biochemistry* **33**, 12042 (1994).
18. S. H. Lee, S. T. Jeong, I. C. Kim, S. M. Byun, *Biochem. Mol. Biol. Int.* **41**, 199 (1997).
19. N. Nassar *et al.*, *Nature Struct. Biol.* **3**, 723 (1996).
20. D. Nihalani, R. Kumar, K. Rajagopal, G. Sahni, *Protein Sci.* **7**, 637 (1998).
21. K. C. Robbins, L. Summaria, R. Wohl, *Methods Enzymol.* **80**, 379 (1981).
22. G. L. Reed, L.-F. Lin, B. Parhami-Seren, P. Kussie, *Biochemistry* **34**, 10266 (1995).
23. V. S. Ganu and E. Shaw, *Int. J. Pept. Protein Res.* **20**, 421 (1982).
24. M. Renatus *et al.*, *EMBO J.* **16**, 4797 (1997).
25. M. Renatus *et al.*, *Biochemistry* **36**, 13483 (1997).
26. K. Tachias and E. L. Madison, *J. Biol. Chem.* **272**, 28 (1997).
27. A. Rabijns, H. L. De Bondt, C. De Ranter, *Nature Struct. Biol.* **4**, 357 (1997).
28. D. K. Grella and F. J. Castellino, *Blood* **89**, 1585 (1997).
29. L. Jespers *et al.*, *Biochemistry* **37**, 6380 (1998).
30. B. Schlott *et al.*, *Biochim. Biophys. Acta* **1204**, 235 (1994).

31. We thank E. Davie, B. W. Matthews, J. D. Capra, and J. Hartsuck for critical reading of this manuscript and N. Cook for technical assistance. Supported by NIH grant HL 60626, grant HR98-029 from Oklahoma Center for the Advancement of Science and Technology, and the resources of the Oklahoma Medical Research Foundation.

2 June 1998; accepted 20 July 1998